

17% CELL EFFICIENCIES ON LARGE BACK-CONTACTED MULTI-CRYSTALLINE SILICON SOLAR CELLS

A.W. Weeber, R. Kinderman, P.C. de Jong, C.J.J. Tool
ECN Solar Energy, P.O. Box 1, 1755 ZG Petten, The Netherlands
Phone: +31 224 564113; Fax: +31 224 568214; email: weeber@ecn.nl

ABSTRACT: In this paper we will demonstrate that back-contacted PUM modules made with industrially applicable processes will result in about 0.7% absolute higher efficiencies than modules manufactured with conventional H-pattern cells. At the cell level, this advantage is about 0.3% absolute, which is almost entirely related to the 2% larger short-circuit current of PUM cells due to less front-side metallization coverage. After interconnection and lamination, an additional 0.5% absolute efficiency gain for PUM was obtained because of the lower series resistance losses in the PUM concept. The more efficient current collection over the cell area and the possibility of using wider interconnection material at the rear are the reasons for the lower resistance losses.

The stability of the in-line PUM process using simple belt furnaces was demonstrated on a batch of more than 350 cells. The average efficiency for PUM cells is 15.8% with a top efficiency of 16.7%. Since lower material quality was used this efficiency will exceed 17% with better Si material.

Keywords: Back Contact, Devices, Module Manufacturing

1 INTRODUCTION

The main trend to reduce the €/W_p costs of multicrystalline silicon (mc-Si) PV technology is by using large and thin wafers. However, processing these large and fragile wafers to modules has several drawbacks:

- going to larger cells will increase the cell's series resistance as a result of longer metallization fingers on the front side, or will result in increased shading losses when going to 3 busbars;
- using a full aluminium rear-side metallization will result in further cell bowing which may lead to breakage during the module manufacturing process;
- larger cells will generate higher currents that will give higher series resistance losses in the interconnection material;
- using traditional tabbing material will cause possible cell breakage at the edges of the fragile thin cell;
- soldering of tabs will result into a highly stressed surface area, which may reduce the yield.

These drawbacks can be overcome by new cell and module concepts such as the PUM concept developed by ECN, as shown in Fig. 1. Series resistance and shading losses for the PUM cell are independent on the cell size, but only depend on the size of the unit cell. The series interconnection of PUM cells can be carried out with hardly any additional series resistance losses. Furthermore, the PUM cell has all contacts on the rear of the cell which makes module manufacturing simpler.

The purpose of the work presented in this paper is to prove on a larger scale that our back-contacted PUM cell-concept will result in higher efficiencies than cells made with the conventional H-pattern concept. This advantage comes out strongest at the module level, i.e., after interconnection and lamination.

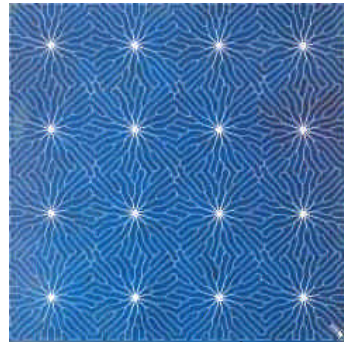


Figure 1: Photograph of a 225 cm² back-contacted PUM cell. The emitter contacts at the rear are realized through 16 laser-drilled vias. Interconnection can be realized at the rear, which makes pick-and-place module manufacturing possible. Furthermore the resistance losses in the module will be very small because of full interconnection from the rear. More details can be found in [1,2].

We prove that in-line processing of high-efficiency mc-Si PUM solar cells is possible. In previous work it was demonstrated that 2% gain in short-circuit current J_{SC} can be obtained by using the PUM concept. This higher J_{SC} is caused by less front-side metallization coverage for PUM. Although the best PUM cells made previously proved to have good efficiencies, it appeared that the process stability was not as good as is needed in production. The efficiency distribution showed a large tail with shunted cells, which resulted in lower efficiencies [3]. Our optimized process, with which we increased the shunt resistance from about 1.5 k Ω cm² to beyond 10 k Ω cm², has resulted in a stable process that proves the possibility of large scale manufacturing of back-contacted solar cells suitable for large cells, with about 0.3% absolute higher cell efficiency [4]. For the module, the efficiency gain is significantly higher [4]. First of all, the more efficient current collection over the cell area and the possibility of using interconnection material that can be much wider than the conventional 2 mm tabs cause PUM modules to result in much lower series-resistance losses than conventional modules. In addition, the PUM cells will be packed more densely in

the module because no tabs are needed in between the cells and because the area for the string matrix is no longer needed.

2 EXPERIMENTAL PUM VERSUS H-PATTERN CELLS

In order to prove the benefits for PUM cells and modules a direct comparison with conventional H-pattern cells was made on 225 cm² 240 μm thick mc-Si wafers from a single commercial supplier. The processing was carried out on groups of neighboring wafers. The reference groups were processed into conventional H-pattern cells while the experimental groups were processed into PUM cells. Both the H-pattern and PUM cells were processed using industrially applicable ECN baseline process steps including a Ag busbar print on the rear (Table I). Junction isolation around the emitter at the rear side was carried out with a 1064nm Nd:YAG laser, i.e., the same laser as was used for making the vias.

Table I: Simple in-line solar cell processing on 225 cm² mc-Si wafers

Process sequence mc-Si cells
1. Laser drilling of 16 holes (PUM cells only)
2. Acidic etching for saw damage removal and surface texturing
3. Homogeneous 60-65 Ω/sq baseline emitter, i.e., double-sided spin-on phosphorous source and infrared-heated metal-belt furnace emitter diffusion
4. SiN _x :H deposition with MicroWave Remote PECVD system
5. Screen-printing of the Ag front side, Ag rear side and Al rear side metallization (Ag rear not in ECN baseline).
6. Simultaneous firing of the front and rear side metallization and Al Back Surface Field (BSF) formation using an infrared heated belt furnace.
7. Emitter edge isolation
8. Laser isolation of the rear-side emitter (PUM cells only)

The processed cells, both H-pattern and PUM, have been further processed into single-cell laminates and full-size modules. The current-voltage (IV) measurements before tabbing, after tabbing and after lamination were carried out using the class A solar simulator at ECN. The measurements on cells and single-cell laminates were performed according to the ASTM-E948 standard [5]. The measurement results have been corrected for spectral mismatch. The modules were characterized with a module flash tester.

3 RESULTS AND DISCUSSION ECN BASELINE

Two complete columns of commercially available wafer, with as size of 12.5×12.5 cm² and thickness of 325 μm, were processed to H-pattern solar cells with a simple industrial process as described in table I, but with full Al rear side. Once every 2 to 3 weeks during a period of 2 years 20 wafers were processed using the same settings for all process equipment. This was done to verify the process stability. The efficiency dependent on the position in the ingot is shown in Fig. 2. The average efficiency obtained over the two columns is 16.0%. Since

a narrow band in efficiency is observed it can be concluded that the ECN baseline process is very stable and can be used as reference process to check the material quality in the PUM experiments.

Nowadays ECN applies 156×156 mm² 240 μm thick mc-Si wafers in its baseline, which also shows good stability.

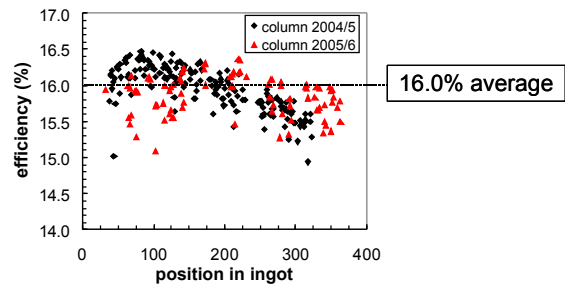


Figure 2: Efficiencies of ECN baselines made in a period of 2 years.

4 RESULTS AND DISCUSSION PUM VERSUS H-PATTERN CELLS

A direct comparison of IV characteristics between H-pattern cells and PUM cells is not very realistic by the different nature of the measurement methods. For H-pattern cells it is known that IV measurement results depend on the probe configuration. For example, the measured *FF* depends on the number of current probes per busbar. We measured the H-pattern cells with multi-probe (8 current probes per busbar) configuration directly on the busbar. The PUM cells were measured using an application-specific measurement chuck (Fig. 3) with 16 current probes for the emitter contacts at the rear and 15 for the base terminals. This will give a first estimate of the difference in cell results between H pattern and PUM cells.

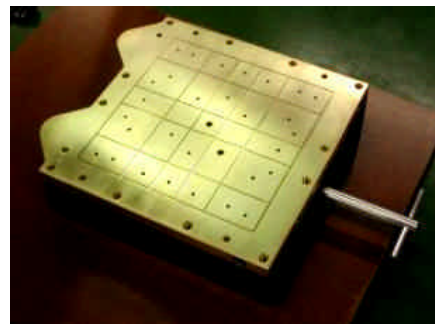


Figure 3: Photograph of the PUM measurement chuck. Current probes (16 to the emitter terminals and 15 to base terminals) contact the cell from the rear.

However, the only realistic comparison between H-pattern cells and PUM cells must be made after interconnection has established. Because of this, all cells were interconnected according to industrially best-applied methods. This implies that H-pattern cells were interconnected with 57 mΩ/m tabbing material. The PUM cells were interconnected with 29 mΩ/m foil. The H-pattern and PUM cell parameters were determined by interconnecting the probe terminals at the tab/foil matrix extension using the four-wire measurement technique.

Single-cell laminates were made using $20 \times 20 \text{ cm}^2$ white tedlar back-sheet foils. Hence, the measured characteristics are the encapsulated cell efficiencies including the benefit of an enlarged white area.

In table II the average IV results both H pattern and PUM cells, and single-cell laminates are presented in table II. Two groups of 6 neighbouring wafers (225 cm^2 ; $240 \mu\text{m}$ thick) were used. These results clearly prove that PUM has advantages over its H-pattern counterpart. PUM laminates perform 5% relative, (0.8% absolute), better than H-pattern cell laminates. This is mainly caused by a 2% larger short-circuit current due to less shading losses, and an additional 3% gain because of the lower resistive losses. If industrial standard $125 \mu\text{m}$ or $150 \mu\text{m}$ thick tabs were used, this effect would even have been larger. Nevertheless, this experiment clearly demonstrates that fill-factor differences between PUM cells and H-pattern cells become larger after interconnection. The somewhat higher V_{OC} value of the PUM cells accounts for an additional 1% gain in efficiency, but its origin is not fully understood.

Table II: IV characteristics averaged over the groups of neighbouring wafers.

Cell type	probe	J_{SC} (mAcm^{-2})	V_{OC} (mV)	FF	η (%)
H	multi	34.2	607	.754	15.7
PUM	multi	34.9	612	.748	16.0
H	tabbed	34.2	608	.720	15.0
PUM	foil	35.0	612	.740	15.9
H	laminated	35.0	609	.724	15.4
PUM	laminated	35.8	613	.739	16.2

A remarkable result is that the encapsulated PUM cell efficiency is about 0.2% absolute higher than the PUM multi-probe measurement. This implies that the current gain due to improved light coupling overcompensates the fill-factor losses due to interconnection. It should be noted that light-coupling effects, the enlarged white area, and mismatch factors may cause some exaggeration of the measured values. The relative values, however, can be compared and show a clear efficiency gain of 0.8% absolute for PUM after laminating single cells.

As described before the baseline process applied typically yields an average efficiency of 16.0% on $125 \times 125 \text{ mm}^2$ H-pattern cells. Apart from wafer quality, there are two additional effects that explain why the H-pattern cells in this experiment stay somewhat behind. Firstly, the up scaling from 125 mm to 150 mm wafers causes additional resistive losses. Secondly, the processing was truly industrial which implies that 6 mm wide Ag busbars were printed on the rear of the H-pattern cells. This leads to some loss of the BSF effect in the busbar regions.

A first step towards industrial application is to make full size modules. 2 groups of 50 neighbouring wafers (225 cm^2 , $240 \mu\text{m}$ thick) were used to make H pattern and PUM cells. The H pattern cells were interconnected using $62 \text{ m}\Omega/\text{m}$ tabbing material, and for the PUM cells $57 \text{ m}\Omega/\text{m}$ foils were used. The IV results can be seen in table III and a picture of both modules is depicted in Fig. 4.

Table III: IV characteristics of full-size H pattern and PUM module.

	I_{SC} (A)	V_{OC} (V)	FF	η (%)	P (W)
H pattern	7.66	22.3	.720	15.2	123
PUM	7.86	22.3	.733	15.8	128



Figure 4: Full size H pattern and PUM module.

Clearly visible are the better results for PUM. A gain of 0.6% absolute (4.4% relative) is observed. The gain in I_{SC} corresponds to that of the single-cell laminates. The gain in FF, however, is somewhat less than on single-cell laminates because foils with a higher resistance were used for full size PUM module. Still FF is about 2% relative better for PUM because 4 foils are used instead of 2 tabs for H pattern cells.

5 EXPERIMENTAL HIGH-EFFICIENCY PUM CELLS

High efficiency PUM cells were made using 225 cm^2 multicrystalline silicon (mc-Si) wafers with a thickness of $270 \mu\text{m}$. The processing used is similar to ECN's in-line baseline based on firing-through $\text{SiN}_x\text{:H}$ and screen-printing. The processing differs from our baseline process by its advanced emitter and several changes of the metallization and firing conditions [6,7,8]. A double-sided emitter was used. On the front side, an advanced high-ohmic homogeneous emitter with a sheet resistivity of about $75 \Omega/\text{sq}$ was made. A low-ohmic emitter on the rear with a sheet resistivity of about $55 \Omega/\text{sq}$ was made simultaneously to minimize shunting and to maximize gettering of impurities. Passivating $\text{SiN}_x\text{:H}$ layers were deposited with an in-line Microwave Remote PECVD system. Cells were metallized using advanced screen-printing. Silver contacts were printed at the front and on the rear. Aluminium was printed on the rear for contacting and formation of the Back-Surface Field (BSF). All contacts were fired simultaneously using an infrared lamp-heated belt furnace. The integral process was optimized to obtain high efficiencies on a large amount of solar cells, thus with a good process stability and high shunt values.

6 RESULTS AND DISCUSSION HIGH-EFFICIENCY PUM CELLS

The results of the high-efficiency PUM process can be found in Table III. The average efficiency of more than 350 cells is 15.8%. The best cell has an efficiency of 16.7%. Simultaneously with the high efficiency PUM group, a few 225 cm^2 H-pattern reference cells processed with our standard baseline. The cell results are shown in Table IV. The multi-probe configuration was used for the

H-pattern cells and the specific PUM chuck of Fig. 3 for measuring the PUM cells.

Table III: Results of a high-efficiency experiment on a total of 354 PUM cells of 225 cm². The PUM cells were measured with the specific PUM chuck as shown in Fig. 3; so not interconnected.

	J_{SC} (mA/cm ²)	V_{OC} (mV)	FF	η (%)
Average	34.6	615	0.743	15.8
Median	34.6	615	0.746	15.9
Champion cell	35.6	618	0.759	16.7

Table IV: IV characteristics averaged over the groups of neighbouring wafers.

	J_{SC} (mA/cm ²)	V_{OC} (mV)	FF	η (%)
H-pattern, standard emitter	33.4	604	.744	15.0
PUM, advanced emitter	34.9	615	.741	15.9

It appeared that the material quality was relatively poor because the H-pattern cells performed 4% relative worse than in the earlier described PUM versus H-pattern experiment. Comparison of the H-pattern multi-probe cell results of Table II with Table IV shows that all cell parameters (V_{OC} , FF and especially J_{SC}) stay behind, leading to an average H-pattern cell efficiency of 15.0% only. This means that using the better material quality will increase the efficiency of the PUM cells with about 4% relative and the champion cell will exceed 17% easily. Applying the process with which we reached 16.8% mc-Si cell efficiency on average [9] will increase the efficiency for PUM even further!

To show the progress made with PUM the efficiency distribution of efficiencies of the complete batch of high-efficiency PUM cells is depicted together with those of previous experiments carried out in 2003 and 2004 (Fig. 5). Furthermore, and the distribution of the 2006 run with which the full size module was made, is added. From this figure it can be seen that the average efficiency since 2003 is increased with more than 2% absolute, and since 2004 with about 0.6% absolute.

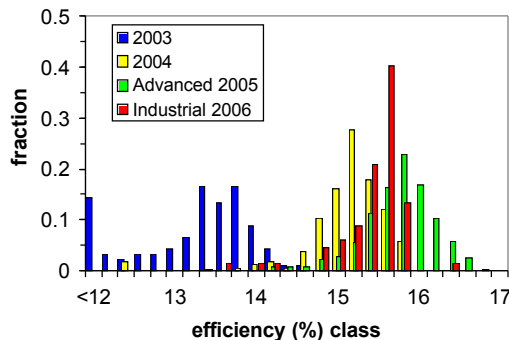


Figure 5: Evolution of PUM cell efficiencies since 2003.

7 CONCLUSIONS

The processing of PUM cells was improved considerably over the last years. This has resulted in an efficiency increase of more than 2% absolute since 2003. The average efficiency of more than 350 PUM cells, with a size of 225 cm², is 15.8% with a top efficiency of 16.7%. These efficiencies were achieved after processing relatively poor-quality wafers into PUM cells. Efficiencies beyond 17% should be possible with better material quality and optimized processing.

The comparison between H-pattern cells with PUM cells is to be treated with delicacy. The only reliable comparison can be achieved after interconnection and/or lamination of the solar cells. It was shown that after lamination (single-cell and full size) PUM achieves a short-circuit current gain of 2-3% in comparison to their H-pattern counterparts due to less shading losses. After interconnection, an additional gain of 2-3% is achieved as a result of the lower resistance losses and the more efficient current collection over the cell area.

It is shown that after interconnection and lamination PUM results in about 0.7% higher absolute efficiency than conventional H-pattern modules. This proves that PUM module efficiencies beyond 16% are possible with PUM cells that are processed using a simple industrial applicable in-line process sequence.

8 ACKNOWLEDGMENTS

Eric Kossen, Martien Koppes, Mario Kloos, Peter Buur and Mark Jansen of ECN are obliged for their technical support.

We gratefully acknowledge the financial support from the Dutch Economy, Ecology and Technology (E.E.T.) program. E.E.T. is an initiative of the Ministry of Economic Affairs, the Ministry of Education, Culture and Science and the Ministry of Public Housing, Physical Planning and Environment.

9 REFERENCES

- [1] J.H. Bultman *et al.*, Proceeding WCPEC-3, Osaka, 2003, 4O-D13-03.
- [2] P.C. de Jong *et al.*, Proceeding 19th EPVSEC, Paris, 2004, 2145.
- [3] F. Granek *et al.*, Proceedings WCPEC-4 Hawaii
- [4] A.W. Weeber *et al.*, WCPEC-4, Hawaii, 2006.
- [5] www.astm.com
- [6] C.J.J. Tool *et al.*, Proceedings 31st IEEE PVSC, Orlando, 2005, 1324.
- [7] C.J.J. Tool *et al.*, Proceedings 20th EPVSEC, Barcelona, 2005, 578.
- [8] C.J.J. Tool *et al.*, Proceedings 15th IPSEC, Shanghai, 2005, 525.
- [9] A.W. Weeber *et al.*, This conference 2EP.1.3.